⌘ *Author's Choice*

Parvulin (Par14), a Peptidyl-Prolyl *cis-trans* Isomerase, Is a Novel rRNA Processing Factor That Evolved in the Metazoan Lineage*

Sally Fujiyama-Nakamura,[a,b,c] Harunori Yoshikawa,[a,b] Keiichi Homma,[d] Toshiya Hayano,[a,e,f] Teruko Tsujimura-Takahashi,[g] Keiichi Izumikawa,[a] Hideaki Ishikawa,[a] Naoki Miyazawa,[a] Mitsuaki Yanagida,[a] Yutaka Miura,[a,g] Takashi Shinkawa,[e,h] Yoshio Yamauchi,[e,h] Toshiaki Isobe,[e,h,i] and Nobuhiro Takahashi[a,e,g,i,j]

Although parvulin (Par14/eukaryotic parvulin homolog), a peptidyl-prolyl *cis-trans* isomerase, is found associated with the preribosomal ribonucleoprotein (pre-rRNP) complexes, its roles in ribosome biogenesis remain undetermined. In this study, we describe a comprehensive proteomics analysis of the Par14-associated pre-rRNP complexes using LC-MS/MS and a knockdown analysis of Par14. Together with our previous results, we finally identified 115 protein components of the complexes, including 39 ribosomal proteins and 54 potential trans-acting factors whose yeast homologs are found in the pre-rRNP complexes formed at various stages of ribosome biogenesis. We give evidence that, although Par14 exists in both the phosphorylated and unphosphorylated forms in the cell, only the latter form is associated with the pre-40 S and pre-60 S ribosomal complexes. We also show that Par14 co-localizes with the nucleolar protein B23 during the interphase and in the spindle apparatus during mitosis and that actinomycin D treatment results in the exclusion of Par14 from the nucleolus. Finally we demonstrate that knockdown of Par14 mRNA decelerates the processing of pre-rRNA to 18 and 28 S rRNAs. We propose that Par14 is a component of the pre-rRNA complexes and functions as an rRNA processing factor in ribosome biogenesis. As the amino acid sequence of Par14 including that in the amino-terminal pre-rRNP binding region is conserved only in metazoan homologs, we suggest that its roles in ribosome biogenesis have evolved in the metazoan lineage. ***Molecular & Cellular Proteomics 8: 1552–1565, 2009.***

Peptidyl-prolyl *cis-trans* isomerases (PPIases)[1] catalyze the rotation about the peptide bond on the amino-terminal side of proline, a step that can be rate-limiting for the folding of newly synthesized proteins (1). PPIases also have the ability to bind many proteins, thereby acting as chaperones; thus, they are believed to control the activity of proteins by regulating their folding, assembly, and intracellular trafficking (2–4). There are three families of PPIases, namely the cyclophilin (CyP), FK506-binding protein, and parvulin families. The CyP and FK506-binding protein families have been well established as targets of the immunosuppressants cyclosporin A and FK506, respectively (5–7).

Together with Pin1, human parvulin (Par14, EPVH) constitutes the parvulin family and has been identified in all hitherto examined human tissues (8, 9). Par14 comprises 131 amino acid residues and has a 35-residue amino-terminal region that does not have sequence similarity to the WW domain (known to bind to phosphorylated serine/threonine-proline bonds in proteins and peptides) of Pin1. Phosphorylation at Ser-19 in this region regulates the subcellular localization and DNA binding activity of Par14; the phosphorylation is required for nuclear localization, and the dephosphorylation is a prerequisite for the binding of the first 25 residues to nuclear DNA (10). The 96-residue carboxyl-terminal domain has a 34.2% sequence identity with the PPIase domain of Pin1. Par14 report-

From the [a]Department of Biotechnology, United Graduate School of Agriculture, Tokyo University of Agriculture and Technology, 3-5-8 Saiwai-cho, Fuchu-shi, Tokyo 183-8509, Japan, [d]Center for Information Biology-DNA Data Bank of Japan, National Institute of Genetics, Research Organization of Information and Systems, Mishima, Shizuoka 411-8540, Japan, [e]Integrated Proteomics System Project, Pioneer Research on Genome the Frontier, Ministry of Education, Culture, Sports, Science and Technology of Japan, Tokyo 102-0075, Japan, [g]Department of Applied Biological Science, Graduate School of Agriculture, Tokyo University of Agriculture and Technology, Tokyo 183-8509, Japan, [h]Department of Chemistry, Graduate School of Sciences and Engineering, Tokyo Metropolitan University, 1-1 Minamiosawa, Hachiouji-shi, Tokyo 192-0397, Japan, and [i]Core Research for Evolutional Science and Technology (CREST), Japan Science and Technology Agency, Sanbancho 5, Chiyoda-ku, Tokyo 102-0075, Japan

⌘ *Author's Choice*—Final version full access.

Received, March 17, 2009

Published, MCP Papers in Press, April 14, 2009, DOI 10.1074/mcp.M900147-MCP200

[1] The abbreviations used are: PPIase, peptidyl-prolyl *cis-trans* isomerase; CyP, cyclophilin; DAPI, 4′,6-diamidino-2-phenylindole; Lys-C, lysyl endopeptidase; Par14, parvulin 14; EPVH, eukaryotic parvulin homolog; PMF, peptide mass fingerprinting; pre-rRNP, preribosomal ribonucleoprotein; RP, ribosomal protein; siRNA, small interference RNA; NCBI, National Center for Biotechnology Information.

edly has a substrate preference for positively charged residues preceding proline but not for phosphorylated Thr or Ser as is the case with Pin1; however, its rate constant for the prolyl *cis* to *trans* isomerization reaction is at least 1,000-fold lower than that of CyPs (9). NMR solution structural analysis has shown that Par14 folds into a $\beta\alpha3\beta\alpha\beta2$ structure, which is essentially identical to that of Pin1 (11). The unstructured 35-residue amino-terminal region contains several basic residues and replaces the WW domain of Pin1 (11). This structural model explains the molecular basis for the preferential substrate specificity of Par14 for positively charged residues preceding proline as well as the putative role of the amino-terminal region as a DNA-binding domain. However, the physiological function of Par14 remains unknown.

We previously reported that Par14 associates with the pre-ribosomal ribonucleoprotein (pre-rRNP) complexes as well as with many proteins that are implicated in the regulation of microtubule assembly or nucleolar reformation during mitosis (12, 13). We have proposed that Par14 is involved in ribosome biogenesis and/or nucleolar reassembly in mammalian cells during the pre- or postmitotic phases of the cell cycle. In the present study, we describe the comprehensive identification of protein components of the Par14-associated pre-rRNP complexes and establish Par14 as a *de facto* component of the pre-rRNP complexes *in vivo*. We also demonstrate that Par14 functions as a ribosomal RNA processing factor in mammalian ribosome biogenesis.

EXPERIMENTAL PROCEDURES

Materials—Mouse fibroblast cell line L929, human embryonic kidney cell line 293EBNA, Lipofectamine, Lipofectamine 2000, Opti-MEM medium, and SuperScript™ were obtained from Invitrogen. Dulbecco's modified Eagle's medium, RPMI 1640 medium, cycloheximide, and non-ionic detergent IGEPAL CA-630 were from Sigma-Aldrich. Antibodies against B23, fibrillarin, and nucleolin were obtained from Santa Cruz Biotechnology (Santa Cruz, CA). Anti-heterogeneous nuclear ribonucleoprotein U was a kind gift from Dr. G. Dreyfuss (University of Pennsylvania). Glutathione-Sepharose 4B and alkaline phosphatase-conjugated anti-mouse and anti-rabbit IgG were purchased from GE Healthcare. Trypsin (sequence grade) was procured from Promega (Madison, WI). Nitro blue tetrazolium/5-bromo-4-chloro-3-indolyl phosphate, Alexa Fluor 488-conjugated rabbit anti-mouse IgG, KOD-Plus polymerase, collagen I-coated Biocoat 8-well culture slides, and a cell counting kit (WST-1) came from Roche Diagnostics, Molecular Probes (Eugene, OR), TOYOBO (Osaka, Japan), BD Biosciences, and Dojindo (Kumamoto, Japan), respectively. All the other reagents used in this study were supplied by Wako Pure Chemical Industries (Osaka, Japan).

Cell Culture—HEK293, 293EBNA, and HeLa cells were grown in Dulbecco's modified Eagle's medium containing 10% fetal bovine serum, 100 IU/ml penicillin G, and 100 μg/ml streptomycin sulfate. L929 and MCF7 cells were grown in RPMI 1640 medium containing 10% fetal bovine serum, 100 IU/ml penicillin G, and 100 μg/ml streptomycin sulfate.

Construction of Expression Vectors for Par14 Deletion Mutants—All the expression plasmids for the Par14 deletion mutants were constructed by introducing PCR-amplified fragments between the BamHI and EcoRI sites downstream of the GST tag in pGEX-2T. Expression constructs of GST-fused full-length Par14 and ΔC2 (residues 1–41) were described previously (12). Plasmids encoding deletion mutants ΔC1 (residues 1–35), ΔC3 (residues 1–44), ΔC4 (residues 1–51), ΔC5 (residues 1–59), and ΔN (residues 36–131) were generated by PCR amplification using the following oligonucleotides: 5′-CAGAATTCTTAGCCACCACCTTTGGGACC-3′ (ΔC1), 5′-GCGAATTCTTATAGAATGTGCTGACCTT-3′ (ΔC3), 5′-CGGAATTCTTAGATTTTGCCATGTTTTTC-3′ (ΔC4), 5′-GGGAATTCTTACTTTAACTTTTCCATGGC-3′ (ΔC5), and 5′-ATCGGATCCAATGCAGTAAAGGTCAGACAC-3′ (ΔN). As the GST fusion ΔN (36–131) mutant could not be cleaved by thrombin protease, the thrombin recognition sequence was introduced as a linker using the oligonucleotide primer 5′-ATCGGATCCCTGGTTCCGCGTGGGTCTAATGCAGTAAAGGTCAGACAC-3′. Proteins were expressed in *Escherichia coli* strain BL21 (DE3). GST fusion protein purification, the GST pulldown assay, and ribonuclease treatment of the Par14 deletion mutant-associated complexes were carried out as described previously (12).

Preparation of a Polyclonal Antibody against Human Par14—Full-length recombinant Par14 was purified essentially as described previously (5). Purified Par14 was used to raise a polyclonal antiserum in rabbit. The anti-Par14 IgG fraction was affinity-purified using recombinant GST-Par14 immobilized to *N*-hydroxysuccinimide-activated Sepharose (Amersham Biosciences).

Immunocytochemistry—293EBNA cells were grown on collagen I-coated 8-well culture slides and fixed with 3.7% formaldehyde in PBS. After washing with PBS-T (PBS containing 0.05% (w/v) Tween 20), the cells were incubated with PBS containing 0.1% (w/v) Triton X-100 for 5 min at room temperature and treated with 3% skim milk in PBS at room temperature. Nucleolar localization of Par14 was monitored by double immunocytostaining. The cells were incubated overnight at 4 °C with the primary antibodies rabbit anti-Par14 and 5 μg/ml goat anti-B23. After washing with PBS-T, the cells were further incubated with FITC-conjugated anti-rabbit IgG and Cy3-conjugated anti-goat IgG (secondary antibodies) for 1 h at room temperature. After washing again with PBS-T, the cells were counterstained with 4′,6-diamidino-2-phenylindole (DAPI). Fluorescence images were visualized with a Bionanoscope (Nikon Engineering, Tokyo, Japan) fitted with a 100× Nikon PlanApo oil immersion objective and two double pass filter sets for fluorescein/DAPI and Texas Red.

Protein Identification by LC-MS/MS and Data Analyses—Par14-associated complexes were digested with lysyl endopeptidase (Lys-C) directly, and the resulting peptides were analyzed using a nanoscale LC-MS/MS system as described previously (14–16). The peptide mixture was applied to a Mightysil-PR-18 (3-μm particles; Kanto Chemical, Osaka, Japan) fritless column (45 mm × 0.150-mm inner diameter) and separated using a 0–40% gradient of acetonitrile containing 0.1% formic acid over 80 min at a flow rate of 50 or 25 nl/min (14). Eluted peptides were sprayed directly into a quadrupole time-of-flight hybrid mass spectrometer (Q-Tof 2, Micromass, Wythenshawe, UK). The peptides were detected in the MS mode to select a set of precursor ions for a data-dependent, collision-induced dissociation mass spectrometric (MS/MS) analysis, and every 4 s the largest four signals selected were subjected to the MS/MS analysis. The MS/MS signals were acquired by MassLynx (Micromass) and converted to text files by ProteinLynx software (Micromass). The database search was performed in triplicate by Mascot (Matrix Science Ltd., London, UK) against the NCBI RefSeq mouse, human, and rat protein sequence databases with the following parameters: variable modifications, oxidation (Met), acetylation, ubiquitination (Lys); maximum missed cleavages, three; peptide mass tolerance, 150 ppm; MS/MS tolerance, 0.5 Da (17, 18). For peptide and protein identification, the search results were processed based on the method described by Shinkawa *et al.* (17). Briefly (i) the candidate peptide sequences were screened with the probability-based molecular weight search (MOWSE) scores that exceeded their thresholds

($p < 0.05$) and with MS/MS signals for y- or b-ions ≥3; (ii) redundant peptide sequences were removed; (iii) each peptide sequence was assigned to a protein that gave the maximal number of peptide assignments among the candidates; (iv) the mouse, human, and rat data sets were combined; and (v) interspecies redundancy of proteins was removed. If necessary, match acceptance of automated batch processes was confirmed by manual inspection of each set of raw MS/MS spectra in which the major product ions were matched with theoretically predicted product ions from the database-matched peptides.

As a control, GST bound to glutathione-Sepharose 4B beads was also pulled down with the nuclear extract. The proteins released from the glutathione-Sepharose beads by the treatment with thrombin (12) were digested with Lys-C, analyzed by the same LC-MS/MS method as used for analysis of the Par14-associated complexes, and subtracted from the proteins identified in the total Par14-associated complexes; thus, those proteins identified in the GST eluate were not included in the Par14-associated proteins unless the quantitative increase was confirmed.

Sucrose Density Gradient Fractionation—At 15 min before harvest, HEK293 cells were treated with 100 μg/ml cycloheximide and incubated at 37 °C. To obtain cytosolic and nuclear extracts, cells were suspended with hypotonic buffer (buffer A (10 mM HEPES, pH 7.8, 10 mM KCl, 10 mM NaF, 1 mM DTT, 2 μg/ml aprotinin, 2 μg/ml pepstatin A, 0.1 mM PMSF) containing 2 mM $MgCl_2$ and 0.05% (w/v) IGEPAL CA-630), incubated for 15 min on ice, and centrifuged at 3,000 × *g* for 5 min, and the resulting supernatant was used as the cytosolic extract. The nuclear pellet was resuspended in buffer A containing 1% (w/v) IGEPAL CA-630, sonicated briefly, and centrifuged at 15,000 rpm for 15 min at 4 °C, and the resulting supernatant was used as the nuclear extract. Each fractionated lysate (200 μl) was applied to a 4.7-ml 10–40% sucrose density gradient in 25 mM Tris-HCl, pH 7.6, 150 mM KCl, 10 mM $MgCl_2$ and centrifuged at 45,000 rpm for 3 h at 4 °C in an MLS-50 rotor (Beckman). A gradient collector (Foxy Jr. from ISCO, Lincoln, NE) was used to record the UV profile and collect 0.25-ml fractions that were precipitated by 10% TCA before SDS-PAGE and immunoblot analyses.

Immunoblotting—Protein samples were denatured at 100 °C in SDS sample buffer, separated by SDS-PAGE, and electrophoretically transferred to an Immobilon-P membrane (Millipore, Billerica, MA). The membranes were incubated either with the primary anti-Par14 serum or affinity-purified antibodies in PBS containing 5% nonfat milk and 0.1% (w/v) Tween 20; washed three times for 5 min with PBS, 0.1% Tween 20; and detected with alkaline phosphatase-conjugated secondary antibodies using the nitro blue tetrazolium/5-bromo-4-chloro-3-indolyl phosphate stock solution according to the manufacturer's instructions (Roche Diagnostics).

RNA Interference Experiments—HEK293 and 293EBNA cells were transfected with siRNAs directed against Par14 (targeting sequences are shown in supplemental Fig. 3A) (Dharmacon, Lafayette, CO) or control non-silencing siRNA (sequence, 5′-AATTCTCCGAACGTGTCACGT-3′; Qiagen, Tokyo, Japan) using Lipofectamine 2000. Cells were collected after transfection and subjected to immunoblotting and RT-PCR. In the analysis of radioisotope-labeled newly synthesized pre-rRNAs, 293EBNA cells were transfected with stealth siRNAs purchased from Invitrogen (supplemental Fig. 3A).

Proliferation Assay—HEK293 cells were transfected with 100 nM siRNA for 4 h, trypsinized, and counted. 10,000 cells were replated onto new 96-well plates and incubated for the indicated times at 37 °C in 5% CO_2. The cell counting kit (Dojindo), which quantifies a disulfonated tetrazolium salt as a chromogenic indicator for NADH by measuring absorbance at 450 nm (formazan), was used to assess living cells according to the manufacturer's instructions. We also used the CellTiter-Glo™ Luminescent Cell Viability Assay kit (Promega) for the proliferation assay, which is a method of determining the number of viable cells in culture based on quantitation of the ATP present, which signals the presence of metabolically active cells.

RT-PCR—Total RNA was isolated from siRNA-transfected cells using the RNasin Total RNA Isolation kit (Promega). Reverse transcription was performed using SuperScript at 42 °C for 60 min followed by 70 °C for 10 min. Aliquots (20 μl) of the reactions containing 1× buffer, 0.5 mM dNTPs, 1 μg of RNA, 25 ng/μl oligo(dT) primer, 5 mM $MgCl_2$, 10 mM DTT, 50 units of SuperScript II reverse transcriptase, and RNaseOUT™ recombinant RNase inhibitor were subjected to 25 cycles of PCR using KOD-Plus polymerase. Each cycle consisted of denaturation at 94 °C for 0.5 min, annealing at 55 °C for 0.5 min, and extension at 72 °C for 2 min, and the final extension reaction was carried out at 72 °C for 10 min. Primers specific for U1 small nuclear ribonucleoprotein-specific C protein (U1RNPC; GenBank™ accession number X12517) were used as a control (22).

Metabolic Labeling and Analysis of RNA Transcripts—siRNA-transfected cells were cultured for 2 days in 35-mm dishes or in 12-well plates before [^{3}H]uridine labeling or metabolic labeling of RNA with L-[*methyl*-^{3}H]methionine, respectively. For [^{3}H]uridine labeling, subconfluent siRNA-transfected 293EBNA cells were incubated with 3 μCi/ml [5,6-^{3}H]uridine (GE Healthcare) for 2 h. After a brief rinse with ice-cold PBS, total RNA was isolated using the RNAgent total RNA isolation system (Promega), and label incorporation was measured by scintillation counting. 2 μg of total RNA was loaded on each lane of a 1% agarose, formaldehyde gel. Separated RNAs on the gel were transferred to a Hybond N^+ membrane (GE Healthcare), which was subsequently dried and sprayed by EN^{3}HANCE (PerkinElmer Life Sciences) and exposed to a Kodak BioMax MS film (Eastman Kodak Co.) for 5 days in a deep freezer. The same transferred membrane was stained with methylene blue for visualizing 28 and 18 S ribosomal RNAs. For metabolic labeling of RNA with L-[*methyl*-^{3}H]methionine, subconfluent siRNA-transfected 293EBNA cells were incubated for 30 min in medium containing L-[*methyl*-^{3}H]methionine (50 μCi/ml; GE Healthcare) after 30-min preincubation in methionine-free medium. The cells were then chased in medium containing a 10-fold excess of nonradioactive methionine after which RNA was isolated using RNAgent, and 5 μg of total RNA was analyzed as described above.

RESULTS

LC-MS/MS Identification of Protein Components Present in the Par14-associated Pre-rRNP Complexes—We have previously described the isolation of Par14-associated pre-rRNP complexes from mouse fibroblast L929 cell nuclear extract (12). We identified 52 proteins involved in ribosome biogenesis, including 26 ribosomal proteins (RPs) and 27 possible trans-acting factors, primarily using the peptide mass fingerprinting (PMF) method with MALDI-TOF/MS after in-gel protease digestion of individual bands excised from SDS-PAGE gels (12). We undertook a more comprehensive examination of the protein components of these Par14-associated pre-rRNP complexes using the shotgun method in which the isolated complexes were digested with Lys-C and analyzed directly by nano-LC-MS/MS (14–16). More than 2,000 MS/MS spectra were obtained from which ~350 peptides were assigned to 88 proteins using the Mascot search software (Table I and supplemental Tables 1–6). When possible, we also performed PMF on the pre-rRNP complexes in parallel with the shotgun analysis (supplemental Tables 4 and 7). The shotgun analysis, together with our previous and present PMF

TABLE I

Par14-associated trans-acting factors putatively involved in ribosome biogenesis

Probable trans-acting factors identified in Par14-associated pre-rRNP complexes are shown. Trans-acting factors involved in ribosome biogenesis are classified into functional groups. For proteins having human and yeast orthologs, the gene names are indicated (obtained by Blink analysis of the NCBI database). Proteins were identified by either LC-MS/MS or MALDI-TOF/MS combined with LC-MS/MS as described in supplemental Tables 1 and 4 and Ref. 12. NCBI accession numbers (GI no.) are shown. Involvement of yeast orthologs in the preribosomal complexes is shown (27). snoRNP, small nucleolar ribonucleoprotein; Brix, biogenesis of ribosome in *Xenopus*; TGF, transforming growth factor; FHA, forkhead-associated; Chr, chromosome; BRCT, BRCA1 carboxyl terminus; RNPs, ribonucleoproteins.

No. in supplemental Table 1	Protein name	Gene symbol	NCBI GI no.	Yeast homolog	Yeast pre-rRNP complex associated	Origin of identification (Ref.)
rDNA transcription-related factor						
1	CCAAT/enhancer-binding protein ζ	*Cebpz*	1705659	Mak21/Noc1	60 S	12
2	MYB-binding protein (P160) 1a	*Mybbp1a*	29179608	Pol5	—[a]	12
3	Sjögren syndrome antigen B	*Ssb*	6678143	Lhp1	—	This study
Box C/D snoRNP						
4	Nucleolar protein 5A	*Nop56*	12844818	Nop56/Sik1	90 S, NSA3	12
5	Nucleolar protein 5	*Nop5*	9256555	Nop5/58	90 S	12
6	WD repeats and SOF1 domain containing	*WDSOF1*	31542526[b]	Sof1	90 S	This study
7	Fibrillarin	*Fbl*	6679755	Nop1	60 S, 90 S	12
8	NHP2 non-histone chromosome protein 2-like 1 (*Saccharomyces cerevisiae*)	*NHP2L1*	4826860[b]	Snu13	Nop58/Mpp10	This study
9	UTP11-like, U3 small nucleolar ribonucleoprotein (yeast)	*Utp11l*	13385534	Utp11	90 S	This study
10	Transducin (β)-like 3	*Tbl3*	26349482	Utp13	90 S	This study
11	Nucleolar protein family 6 (RNA-associated)	*Nol6*	18539460	Utp22	90 S	This study
Box H/ACA snoRNP						
12	Dyskeratosis congenita 1, dyskerin homolog (human)	*Dkc1*	20145499	Cbf5	90 S	This study
13	Nucleolar protein family A, member 3 (H/ACA small nucleolar RNPs)	*Nop10*	63691694	Nop10	H/ACA snoRNP	This study
RNA helicase						
14	DEAD (Asp-Glu-Ala-Asp) box polypeptide 5	*DHx15*	51262	Dbp2	60 S	12
15	DEAH (Asp-Glu-Ala-His) box polypeptide 9	*Dhx9*	24429590	—	—	This study
16	DEAH (Asp-Glu-Ala-His) box polypeptide 15	*DDX15*	9624452[b]	Prp43	—	12
17	DEAD (Asp-Glu-Ala-Asp) box polypeptide 18	*Ddx18*	13385342	Has1	90 S, 60 S	12
18	DEAD (Asp-Glu-Ala-Asp) box polypeptide 21 (RNA helicase II/Gu)	*Ddx21*	13959325	Dbp1/Lph8	—	This study
19	DEAD (Asp-Glu-Ala-Asp) box polypeptide 24	*Ddx24*	9931362	Mak5	60 S	12
20	DEAD (Asp-Glu-Ala-Asp) box polypeptide 27	*Ddx27*	15030137	Drs1	60 S	12
21	DEAH (Asp-Glu-Ala-His) box polypeptide 30	*Dhx30*	19111156	Prp2/Rna2	—	This study
22	DEAD (Asp-Glu-Ala-Asp) box polypeptide 48	*Eif4a3*	20149756	Tif1	—	This study
23	DEAD (Asp-Glu-Ala-Asp) box polypeptide 56	*Ddx56*	26345783	Dbp9	60 S	12
RNA modification enzymes						
24	FtsJ homolog 3 (*E. coli*)	*Ftsj3*	13384672	Spb1	60 S	12
25	Nucleolar protein 1	*Nol1*	13938070	Nop2/Yna1	60 S	12
WD repeat						
26	Block of proliferation 1	*Bop1*	7304931	Erb1	60 S	12
27	WD repeat domain 12	*Wdr12*	10946614	Ytm1	60 S	12
28	PWP1 homolog (*S. cerevisiae*)	*Pwp1*	12845102	Pwp1	90 S, 60 S	This study

TABLE I—*continued*

No. in supplemental Table 1	Protein name	Gene symbol	NCBI GI no.	Yeast homolog	Yeast pre-rRNP complex associated	Origin of identification (Ref.)
BRIX family proteins (σ^{70}-like motif)						
29	Brix domain-containing 1	*Bxdc1*	19263816	Rpf2	60 S	12
30	Brix domain-containing 2	*BXDC2*	55770900[b]	Brx1	60 S	This study
31	Brix domain-containing 5	*Bxdc5*	12843509	Rpf1	60 S	This study
32	Peter pan homolog (*Drosophila*)	*Ppan*	21704228	Ssf1	60 S	This study
RNA-binding protein						
33	RNA binding motif protein 28	*RBM28*	8922388	Nop4/77	60 S	12
34	Nucleolin	*Ncl*	13529464	Nsr1/She5	—	12
35	Nucleolar and coiled body phosphoprotein 1	*NOLC1*	4758860[b]	Srp40	snoRNP	This study
36	RNA binding motif protein 13	*MAK16*	31543091[b]	Mak16	60 S	This study
37	RNA binding motif protein 28	*Rbm28*	12859434	Nop4/77	60 S	This study
38	Poly(A)-binding protein, cytoplasmic 1	*Pabpc1*	6679197	Pab1	—	This study
39	DNA segment, Chr 19, Brigham and Women's Genetics 1357 expressed	*D19Bwg1357e*	25032232	Puf6	60 S	This study
40	Mki67 (FHA domain) interacting nucleolar phosphoprotein	*Mki67ip*	13774097	Nop15	60 S	12
41	Nucleophosmin (nucleolar phosphoprotein B23, numatrin)	*NPM1*	15214852[b]		—	This study
Others						
42	Ribosome-binding protein 1	*Rrbp1*	12860388	Nup116	Complex subunit	This study
43	Nucleolar complex-associated 2 homolog (*S. cerevisiae*)	*Noc2l*	18044823	Noc2/Rix3	60 S	This study
44	Nucleolar complex-associated 3 homolog (*S. cerevisiae*)	*Noc3l*	23956108	Noc3	60 S	This study
45	GTP-binding protein 4	*Gtpbp4*	17368619	Nog1	60 S	12
46	Guanine nucleotide-binding protein-like 2 (nucleolar)	*Gnl2*	13096930	Nog2	60 S	12
47	Novel nuclear protein 1	*Nop52*	21431818	Rrp1	60 S	12
48	RIKEN cDNA 5730427N09, TGF β-inducible nuclear protein 1	5730427N09Rik	10946994	Nsa2	60 S	This study
49	Ribosomal L1 domain-containing 1	*Rsl1d1*	21707758	Cic1/Nsa3	90 S, 60 S	12
50	RRS1 ribosome biogenesis regulator homolog (*S. cerevisiae*)	*Rrs1*	14719402	Rrs1	60 S	12
51	EBNA1-binding protein 2	*Ebna1bp2*	12841070	Ebp2	60 S	12
52	RIKEN cDNA 2610012O22 gene	*Mrto4*	12847477	Mrt4	60 S	12
53	*S. cerevisiae* Nip7p homolog, RIKEN cDNA 1110017C15 gene	*Nip7*	12852038	Nip7	60 S	This study
54	Pescadillo homolog 1, containing BRCT domain (zebrafish)	*Pes1*	11875634	Nop7/Yph1	60 S	12

[a] —, their associated pre-rRNP complexes have not been identified.
[b] GI number identified from the human database.

analyses, identified 115 proteins in the Par14-associated pre-rRNP complexes. Of these, 39 were RPs consisting of 29 large subunit RPs, two P proteins (P0 and P3), and eight small subunit RPs (supplemental Table 2), whereas 76 were non-RPs (Table I and supplemental Table 3). Of the 76 non-RPs, 54 were putative trans-acting factors involved in ribosome biogenesis with homology to yeast trans-acting factors (Table I and supplemental Table 1). Based on the availability of antibodies, we selected three proteins, namely heterogeneous nuclear ribonucleoprotein U, fibrillarin, and nucleolin, and confirmed their presence in the Par14-associated pre-rRNP complexes using immunoblot (supplemental Fig. 1). The present analysis added 27 new putative trans-acting factors involved in mammalian ribosome biogenesis in addition to the 27 previously reported as components of the Par14-associated pre-rRNP complexes (12). In addition, 22 non-RPs having unknown functions in ribosome biogenesis were identified in the Par14-associated pre-rRNP complexes. These proteins were classified into five functional groups (supplemental Table 3).

Endogenous Par14 Localizes Mostly to the Nucleolus during Interphase and in the Spindle Apparatus during Mitosis—As the above results indicated that Par14 binds to the pre-rRNP complexes, Par14 should localize to the nucleolus, the site of ribosome biogenesis. Our previous analysis using FLAG-tagged Par14 showed that it was dispersed mainly in the nucleus. To examine whether endogenous Par14 actually localizes to the nucleolus, we raised a polyclonal antibody

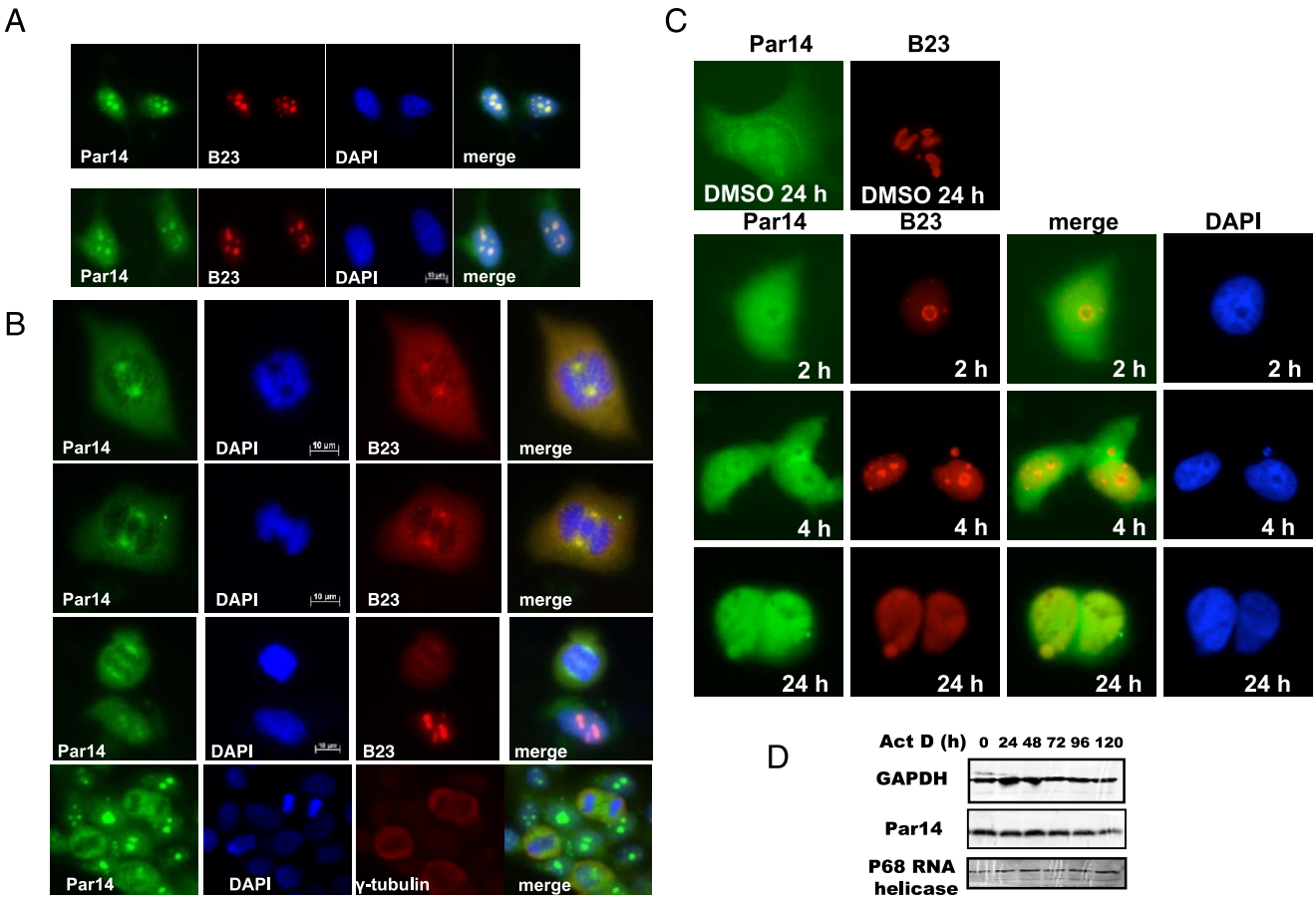

FIG. 1. **Cellular localization of endogenous Par14.** *A*, localization of endogenous Par14 in quiescent MCF7 (*upper*) and HeLa (*lower*) cells. *DAPI*, DAPI image showing the position of the nuclei. *Par14*, corresponding immunolocalization of endogenous Par14. *B23*, corresponding images stained for B23 indicating nucleoli. *Merge*, merge of Par14, B23, and DAPI. *B*, localization of Par14 during mitosis of HeLa cells. The same abbreviations as in *A* are used. γ-*Tubulin* and *B23*, images stained for γ-tubulin and B23 during mitosis indicating the spindle apparatus. *C*, 293EBNA cells were treated with 50 ng/ml actinomycin D for the indicated periods and stained for analysis by indirect immunofluorescence (Par14 in *green*; B23 in *red*). *DMSO*, treated with DMSO for 24 h. *D*, total proteins from cells treated for longer periods with actinomycin D (*Act D*) analyzed by immunoblotting with antibodies against the proteins whose names are indicated to the *left*. *GAPDH*, glyceraldehyde-3-phosphate dehydrogenase.

against Par14 (anti-Par14) (see "Experimental Procedures") and confirmed its specificity by immunocytochemistry (supplemental Fig. 2A) and immunoblotting (supplemental Fig. 2B). Immunocytochemical analysis revealed that endogenous Par14 was in the cytoplasm and the nucleus but was clearly concentrated in foci, co-localizing with the nucleolar-specific protein B23 in quiescent cells (Fig. 1*A*), indicating that Par14 localizes to the nucleolus of those cells during interphase. In addition, Par14 co-localized almost completely with B23 in the spindle apparatus during mitosis (Fig. 1*B*), which is typical of trans-acting factors involved in ribosome biogenesis (19–22). Furthermore upon treatment with actinomycin D, Par14 was excluded from the nucleolus and was observed to disperse throughout the nucleoplasm much faster than did B23 (Fig. 1*C*), whereas the amount of Par14 in the cells was not affected by actinomycin D (Fig. 1*D*). These results suggest that in all respects Par14 behaves as a component of the pre-rRNP complexes *in vivo*.

Endogenous Par14 Is Present in Nuclear Pre-40 S and Pre-60 S Ribosomal Fractions—Anti-Par14 was used to examine the presence of endogenous Par14 in preribosomal particles. A single SDS-PAGE band (designated Par14-a) was detected in the cytoplasmic extract at ~14-kDa molecular mass, whereas two protein bands were identified in the nuclear extract at ~14 kDa (Par14-a) and a slightly smaller molecular mass (labeled as Par14-b) (Fig. 2*A*). As treatment of the cytoplasmic extract with λ-phosphatase shifted the gel migration of Par14-a toward that of Par14-b, we reason that endogenous Par14 exists in both phosphorylated (Par14-a) and unphosphorylated (Par14-b) forms (Fig. 2*B*).

Sucrose density gradient ultracentrifugation was used to fractionate cytoplasmic and nuclear extracts prepared from HEK293 cells, and each fraction was subjected to immunoblotting with anti-Par14. Cytoplasmic Par14 was exclusively detected in non-ribosomal fractions having lower density (Fig. 2*C*; fractions 1–6), whereas nuclear Par14 was detected not only in

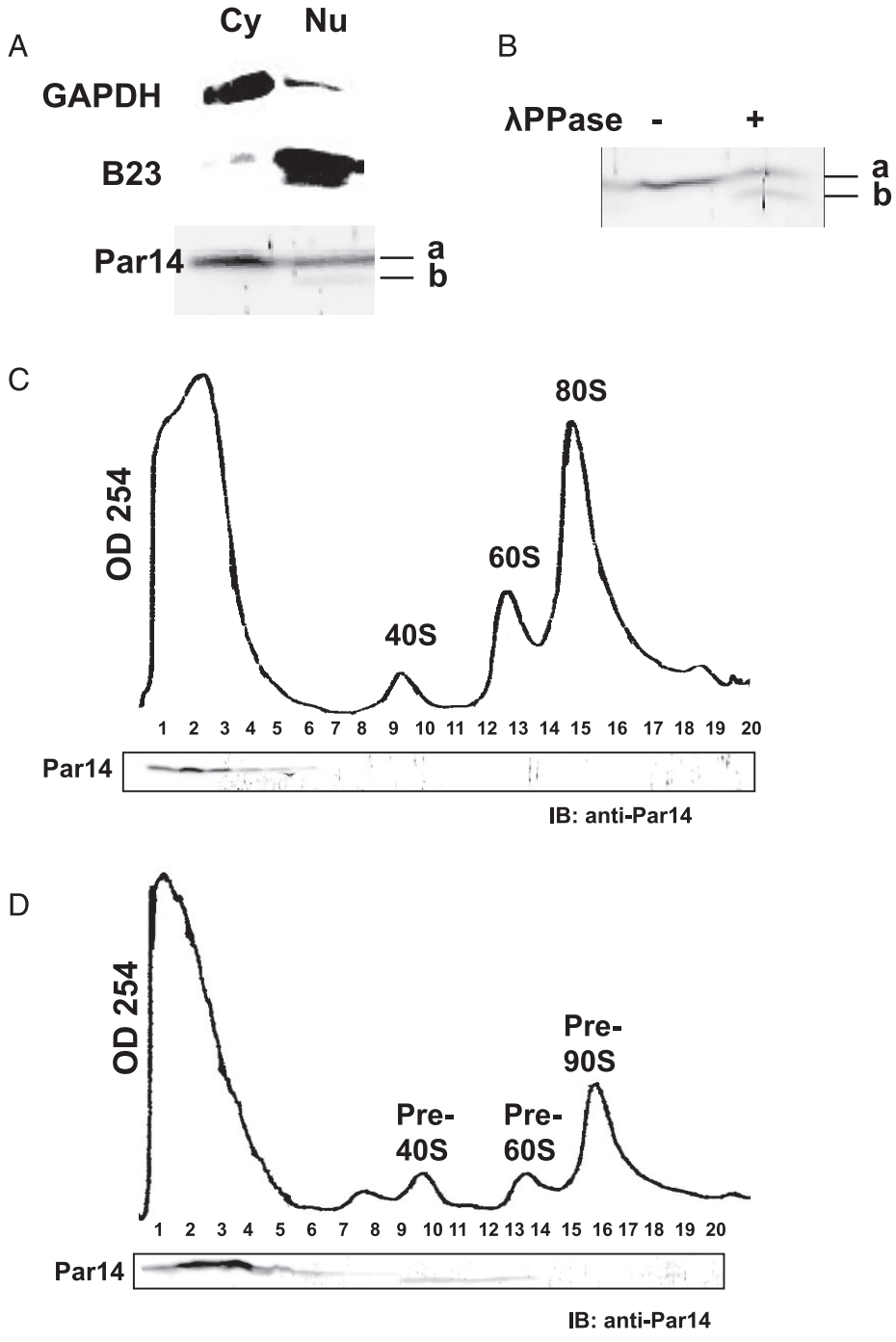

FIG. 2. **Presence of endogenous Par14 in preribosomal particles.** *A*, cytosolic (*Cy*) and nuclear (*Nu*) extracts obtained from HEK293 cells were subjected to SDS-PAGE and immunoblotting with antibodies against glyceraldehyde-3-phosphate dehydrogenase (*GAPDH*), B23, or Par14. *a*, Par14-a; *b*, Par14-b. *B*, cytosolic extracts treated with (+) or without (−) λ-phosphatase (λ*PPase*) were analyzed by immunoblotting (*IB*). *a*, Par14-a; *b*, Par14-b. *C*, cytosolic extract was subjected to ultracentrifugation on a 10–40% sucrose gradient, separated into 20 fractions, and monitored by absorbance at 254 nm. Each fraction was analyzed by immunoblotting using anti-Par14. Ribosomal fractions corresponding to 40, 60, and 80 S particles are indicated *above* the corresponding fractions. *D*, nuclear extract was separated by ultracentrifugation as above. Prior to ultracentrifugation, the cytosolic (*C*) and nuclear (*D*) extracts were adjusted to the same amount by measuring absorbance at 280 nm. Preribosomal fractions corresponding to pre-40 S, pre-60 S, and pre-90 S particles are indicated *above* the corresponding fractions.

non-ribosomal fractions but also in pre-40 S and pre-60 S ribosomal fractions (Fig. 2*D*; fractions 8–13). Intriguingly the Par14 in non-ribosomal fractions corresponded to Par14-a (phosphorylated form), whereas that in pre-40 S and pre-60 S fractions matched Par14-b (unphosphorylated form). Our observations thus suggest that only unphosphorylated Par14 associates with the pre-rRNP complexes in the nucleus.

Knockdown of Par14 Reduces the Production of 18 and 28 S rRNAs—To clarify the involvement of Par14 in ribosome biogenesis, we examined the effects of RNA interference-mediated Par14 knockdown on cell growth and pre-rRNA processing. Two small interfering RNAs (si-169 and si-287) were used to knock down Par14 mRNA in HEK293 cells (supplemental Fig. 3A). Both siRNAs, when transfected individually, reduced Par14 mRNA and protein by more than 80% compared with cells transfected with negative control siRNA after 3 days of transfection as detected by RT-PCR (supplemental Fig. 3B) and immunoblotting with anti-Par14 (supplemental Fig. 3, C and D). Interestingly when performing the knockdown experiments we detected an alternatively spliced

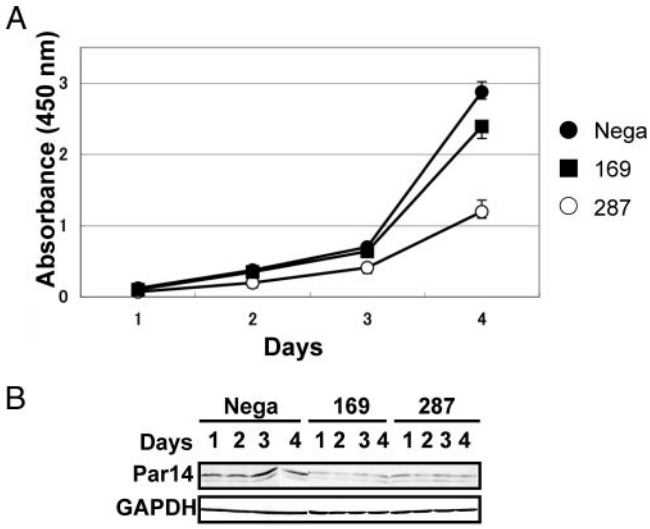

FIG. 3. **Suppression of cell growth by knockdown of Par14 mRNA.** *A*, HEK293 cells were transfected for 6 h with siRNA, trypsinized, and counted. Cells (5×10^3) were seeded on 96-well plates, and subsequent growth was monitored using a cell counting kit (Dojindo). The values indicated are averages (±S.D.) of four independent experiments. Cells transfected with a negative control siRNA (*Nega*) were used as a control for the proliferation rate. *B*, immunoblotting was used to determine the expression level of Par14 in the cells used for the proliferation assay. *GAPDH*, glyceraldehyde-3-phosphate dehydrogenase.

form of Par14 mRNA in both mock- and siRNA-treated cells (supplemental Figs. 3, E–I) whose function is unknown at present. As Par14 knockdown suppressed cell growth (Fig. 3, *A* and *B*), appropriate expression of Par14 is necessary for normal cell growth.

We also knocked down Par14 mRNA with stealth-Par14si (supplemental Fig. 3A and Fig. 4*A*) and examined incorporation of [^{3}H]uridine in newly synthesized RNAs in 293EBNA cells. This siRNA effectively suppressed cell growth as well (supplemental Fig. 3, J and K); the magnitude of the effects on cell growth upon Par14 knockdown was comparable to that upon the knockdown of B23 (a well known trans-acting factor involved in mammalian ribosome biogenesis) with stealth-B23si (supplemental Fig. 3, A, L, and M). Although the stealth-Par14si did not significantly alter the [^{3}H]uridine incorporation when compared with that of the 293EBNA cells treated with negative control stealth-siRNA (Fig. 4*B*), metabolic labeling using [^{3}H]uridine showed that the deficiency of Par14 slowed the production of 18 S as well as 28 S rRNAs (Fig. 4, *C* and 4*D*). Pulse-chase analysis using [^{3}H]methionine verified that the deficiency of Par14 reduced the production of the two rRNAs (Fig. 4, *E* and *F*). These results indicate that Par14 is required for the proper production of 18 and 28 S rRNAs.

The Amino-terminal Region (Residues 36–41) of Par14 Is Prerequisite for Its Association with the Pre-rRNP Complexes—We demonstrated previously that the 41-residue amino-terminal region was responsible for the association of Par14 with the pre-rRNP complexes (12). Considering that the 25 amino-terminal residues of Par14 constitute a DNA-binding domain (11), we examined whether the same region is responsible for its association with both DNA and the pre-rRNP complexes. In addition to the previously constructed ΔC2 mutant (residues 1–41), we prepared five domain mutants (ΔC1, ΔC3, ΔC4, ΔC5, and ΔN1) that were fused to GST with a thrombin cleavage site (Fig. 5, *A* and *B*) and performed a GST pulldown assay for each of the domain mutants using the nuclear extract of mouse L929 cells (Fig. 5*C*). In contrast to the domain mutant ΔC2 (residues 1–41), which was found associated with pre-rRNP complexes in agreement with our previous report (12), the ΔC1 mutant (residues 1–35) containing the DNA binding region (residues 1–25) (14) did not bind to the pre-rRNP complexes (Fig. 5*C*). In addition, the ΔC3 (residues 1–45) and ΔC4 (residues 1–51) domain mutants associated with the pre-rRNP complexes in an RNA-dependent manner, whereas ΔC5 (residues 1–59) was found in association with a number of proteins RNA independently. Meanwhile the domain mutant ΔN1 (residues 36–131) did not associate with the pre-rRNP complexes (Fig. 5*C*), although it shares the 36–41 region with ΔC2. These findings suggest that both the amino acid residues 36–41 and the amino-terminal 35 residues are required for the binding of Par14 to the pre-rRNP complexes, although we cannot exclude the possibility that the presence of the residues 42–131 inhibits the association of the residues 36–41 with the pre-rRNP complexes. We also confirmed the requirement of the region 36–41 for the association with the pre-rRNP complexes using the nuclear extract of human 293EBNA cells (Fig. 5*D*). Thus, the region 36–41 is a prerequisite for the association of Par14 with the pre-rRNP complexes, and distinctive regions of Par14 are probably used for its association with DNA and the pre-rRNP complexes. These results demonstrate that the amino-terminal 41 resides of Par14 are essential for its role in ribosome biogenesis.

DISCUSSION

Our comprehensive identification of the protein constituents of the Par14-associated pre-rRNP complexes by a shotgun method using LC-MS/MS increased the number of putative trans-acting factors from 27 to 54 (Table I). This refined analysis indicated that Par14 has the ability to associate with a wide range of trans-acting factors whose yeast homologs are found in many different pre-rRNP complexes and that Par14 associates with multiple pre-rRNP complexes formed at various stages of mammalian ribosome biogenesis (Table I). We confirmed this by showing that endogenous Par14 was present in both pre-40 S and pre-60 S ribosomal fractions from sucrose gradient ultracentrifugation of nuclear extract (Fig. 2). In addition, Par14 co-localized with nucleolar B23 during interphase and in the spindle apparatus during mitosis (Fig. 1, *A* and *B*), suggesting that Par14 functions as part of the pre-rRNP complexes during most of the cell cycle. In support of this notion, treatment with actinomycin D, a selec-

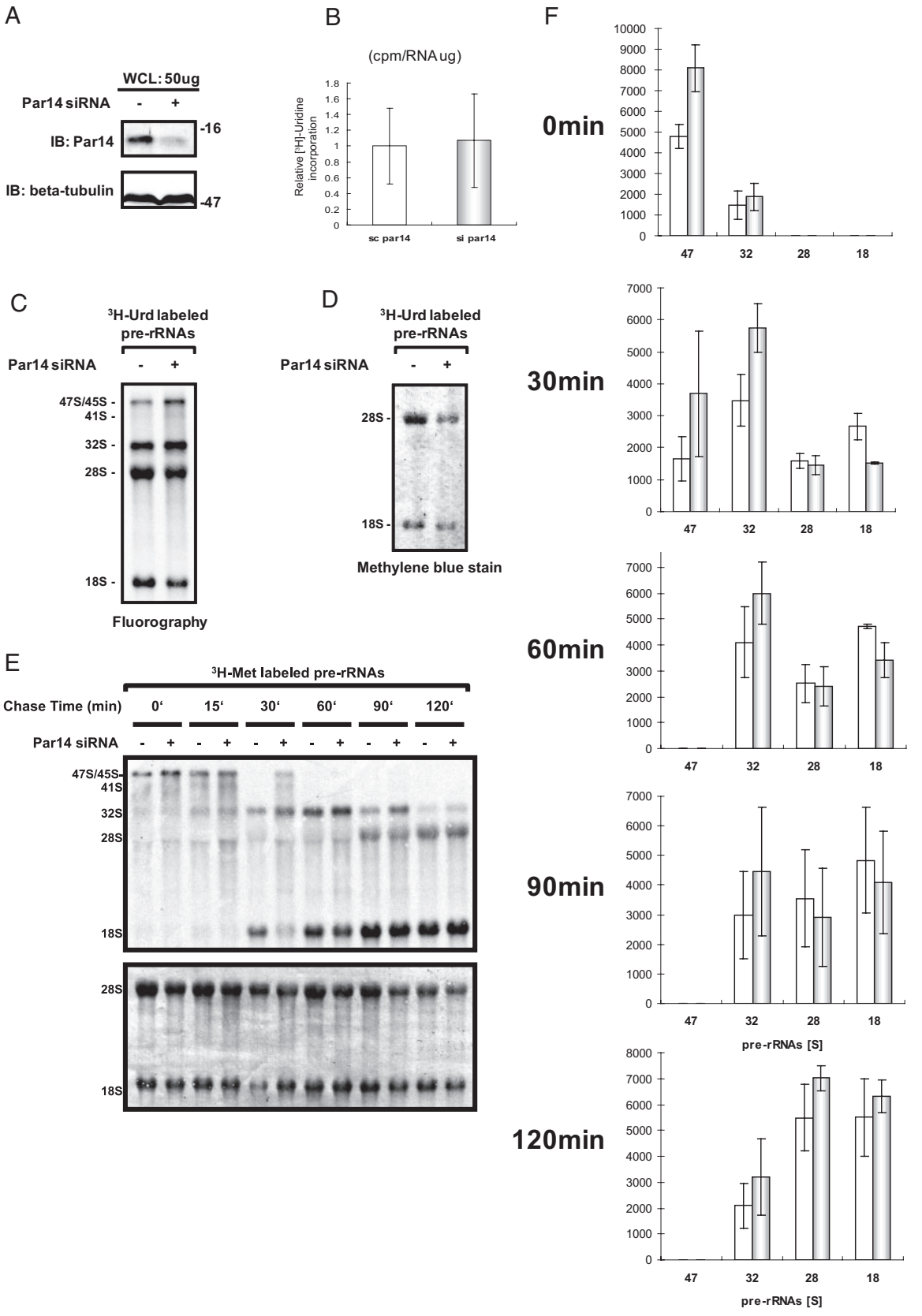
A
WCL: 50ug
Par14 siRNA - +
IB: Par14
-16
IB: beta-tubulin
-47
B
(cpm/RNA ug)
Relative [3H]-Uridine incorporation
sc par14
si par14
C
3H-Urd labeled pre-rRNAs
Par14 siRNA - +
47S/45S
41S
32S
28S
18S
Fluorography
D
3H-Urd labeled pre-rRNAs
Par14 siRNA - +
28S
18S
Methylene blue stain
E
3H-Met labeled pre-rRNAs
Chase Time (min) 0' 15' 30' 60' 90' 120'
Par14 siRNA - + - + - + - + - + - +
47S/45S
41S
32S
28S
18S
28S
18S
F
0min
30min
60min
90min
120min
47 32 28 18
pre-rRNAs [S]

tive inhibitor of rRNA synthesis, resulted in the exclusion of Par14 from the nucleolus (Fig. 1*C*). The results of this study together with our previous report that the Par14-associated pre-rRNP complexes contain pre-rRNA species (12) established the association of Par14 with the pre-rRNP complexes both *in vitro* and *in vivo*. Consistent with the idea that that Par14 is a pre-rRNA processing factor involved in mammalian ribosome biogenesis, Par14 deficiency slowed cell growth (Fig. 3*A*) and reduced the production of 18 and 28 S rRNAs (Fig. 4, *C* and *E*). To our knowledge, Par14 is the first PPIase that was shown to be a pre-rRNA processing factor in any species.

Although ribosome biogenesis has been studied extensively in yeast cells, no Par14 homologs was found in the identified trans-acting factors involved in yeast ribosome biogenesis. In fact, yeast has only one PPIase belonging to the parvulin family, Ess1, whose mammalian homolog is Pin1; however, Ess1 has not been shown to be involved in ribosome biogenesis in yeast cells so far. To inquire into possible evolutionary conservation of the role of Par14 in pre-rRNP processing paying attention to the amino-terminal domain that associates with the pre-rRNP complexes, we first searched for protein sequences that align to the amino-terminal 45-amino acid sequence of human Par14 in the UniRef100 database (version 14.0) containing over 6.2 million entries using BlastP (E-value $<$ 0.01 without SEG filtering) and got 30 non-fragmental sequences. Because the amino acid sequence NAVKVR (residues 36–41) of Par14 is a prerequisite for its association with pre-rRNP complexes (Fig. 5), we next examined which of the 30 proteins have at least three residues in 60-residue amino-terminal regions matching the hexaresidue pattern. We found 21 entries, all of which had more than or equal to four amino acid residues matching the NAVKVR pattern. Finally we confirmed that all of those sequences are aligned to the entire amino acid sequence of Par14 using BlastP with the same conditions as above (Fig. 6). PPIases with significant homology to Par14 were found exclusively in metazoans higher than *Caenorhabditis* (Fig. 6). The results suggest that these PPIases have the ability to associate with the pre-rRNP complexes, and this in turn implies that the roles of Par14 in ribosome biogenesis have evolved in the metazoan lineage.

Although no homologs of B23 (nucleophosmin) have been found in yeast, it is a well known trans-acting factor that is involved in 60 S large subunit production in mammalian cells. B23 homologs were present in amphibian and higher organisms, *e.g. Xenopus laevis* (supplemental Fig. 4), indicating its role in ribosome biogenesis in these species. These examples imply that cell lineage- or species-specific trans-acting factors involved in ribosome biogenesis are common among different species. Recently Young *et al.* (24) showed that deficiency of Runx2, a Runt-related cell-specific transcription factor, enhanced rRNA synthesis and proposed that lineage-specific control of ribosomal biogenesis may be a fundamental function of transcription factors that govern cell fate. Par14 and B23 may regulate ribosome biogenesis at the post-transcriptional level in a cell lineage-specific manner.

How is Par14 involved in pre-rRNA processing during ribosome biogenesis? One possible role is involvement in the recruitment of trans-acting factors and/or the direction of factors to appropriate pre-rRNP complexes. This proposed role is based on our result that Par14 is associated with pre-rRNP complexes at the 41-residue amino-terminal domain distinct from the carboxyl-terminal PPIase domain. The amino-terminal region may act as an anchor to the pre-rRNP complexes, whereas the carboxyl-terminal PPIase domain may capture trans-acting factors and/or ribosomal proteins and transfer them to the pre-rRNP complexes and/or sequester them from the complexes. The PPIase activity of Par14 may be required for those actions. This proposal suggests that Par14 may control the recruitment of trans-acting factors to appropriate pre-rRNP complexes by binding to them and catalyzing their conformational changes.

The proposed role of Par14 in ribosome biogenesis is based on the discovery that Par14 uses one amino-terminal region (residues 1–25) to associate with DNA and another (residues 1–41; the presence of residues 36–41 is a prerequisite) to associate with the pre-rRNP complexes (Fig. 5, *A–D*). Because Par14 apparently accumulates around chromosomes during mitosis (Fig. 1*B*), this result suggests that it may also participate in the redistribution of the pre-rRNP complexes associated with ribosome biogenesis and/or nucleolar reassembly during pre- or postmitotic phases of the cell cycle as we proposed previously (12). The finding that a yeast homolog (Nop15p) of a component of the Par14-associated pre-rRNP complexes (the product of the open reading frame

FIG. 4. **Par14 deficiency alters rRNA synthesis and its processing *in vivo*.** *A*, immunoblot (*IB*) analysis of whole cell extracts (*WCL*) prepared from either stealth-siRNA (negative control)-treated (−) or stealth-Par14si (Par14 siRNA)-treated cells (+) incubated with either anti-Par14 antibody (*IB: Par14*) or anti-β tubulin antibody (*IB: β-tubulin*). *B*, relative [^{3}H]uridine incorporation in total RNA. Newly synthesized RNA was measured by [^{3}H]uridine incorporation into total RNA by scintillation counting (cpm) and normalized to 1 μg of RNA. *C*, [^{3}H]uridine labeling of pre-rRNA synthesis by fluorography. Newly synthesized pre-rRNA and processed rRNAs were detected by [^{3}H]uridine labeling for 2 h after 120-h treatment of 293EBNA cells with Par14 siRNA (+) or control (−). *D*, 2 μg of total RNA extracted from Par14 siRNA-treated or control siRNA-treated cells was loaded. 28 and 18 S rRNAs were detected by methylene blue. *E*, pulse-chase experiment. RNA synthesis was measured by L-[*methyl*-^{3}H]methionine incorporation using fluorography at 0, 15, 30, 60, 90, and 120 min after a 30-min incubation of cells in culture medium containing L-[*methyl*-^{3}H]methionine. 5 μg of total RNA was loaded into each lane. The same blot was stained with methylene blue for estimation of rRNA levels. *F*, the values are the averages of four independent pulse-chase experiments of the type presented in *E* by densitometry quantification. *Error bars* signify S.D.

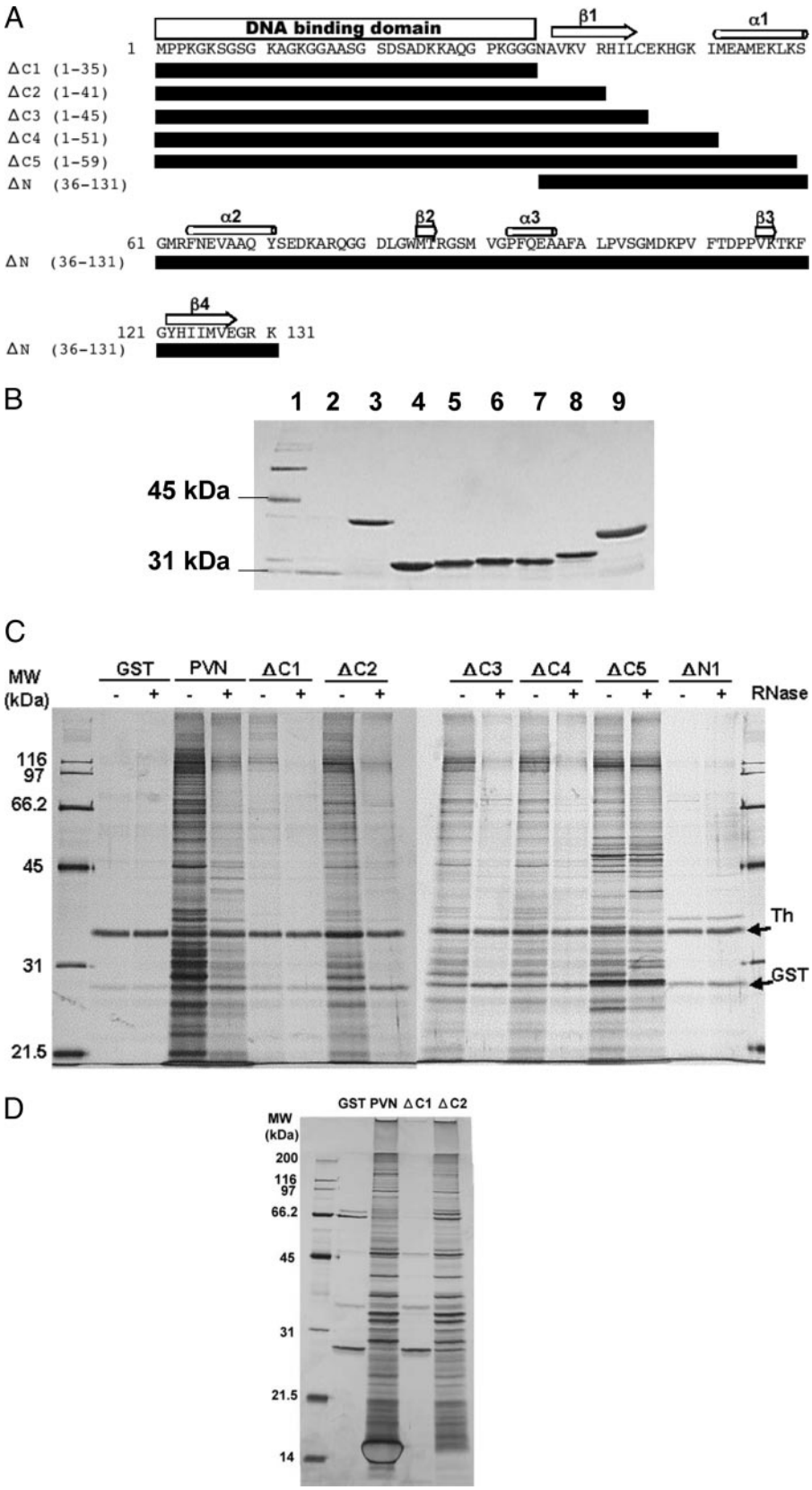

FIG. 5. **Requirement of residues 36–41 of Par14 for its association with the pre-rRNP complexes.** *A*, six truncated mutants, ΔC1, ΔC2, ΔC3, ΔC4, ΔC5, and ΔN1, were constructed as schematically shown *under* the amino acid sequence of Par14. The residues comprising each mutant are indicated in *parentheses*. A GST tag (not shown) was added to the amino terminus of each peptide. The locations of the DNA-binding domain, α-helices, and β-sheets are indicated *above* the corresponding amino acid sequences. *B*, each of the truncated mutants was expressed in *E. coli*, purified on a glutathione-Sepharose column, and analyzed by SDS-PAGE. *Lane 1*, molecular mass markers; *lane 2*, GST; *lane 3*, full-length Par14; *lane 4*, ΔC1; *lane 5*, ΔC2; *lane 6*, ΔC3; *lane 7*, ΔC4; *lane 8*, ΔC5; *lane 9*, ΔN1. *C*, SDS-PAGE of proteins from L929 cell nuclear extract pulled down by GST-Par14 and its truncated mutants. The proteins or mutants ("baits") used for the pulldown analysis are indicated *above* each set of lanes with (+) or without (−) RNase. Molecular mass markers were run in peripheral lanes. *Arrows* to the *right* indicate thrombin (*Th*), which was used to elute the proteins associated with affinity bait, and GST, which was generated upon cleavage of the GST-fused peptides with thrombin. *D*, SDS-PAGE of the proteins from 293EBNA cell nuclear extract pulled down by GST-Par14 ("*GST*"), full-length Par14 ("*PVN*"), ΔC1, or ΔC2.

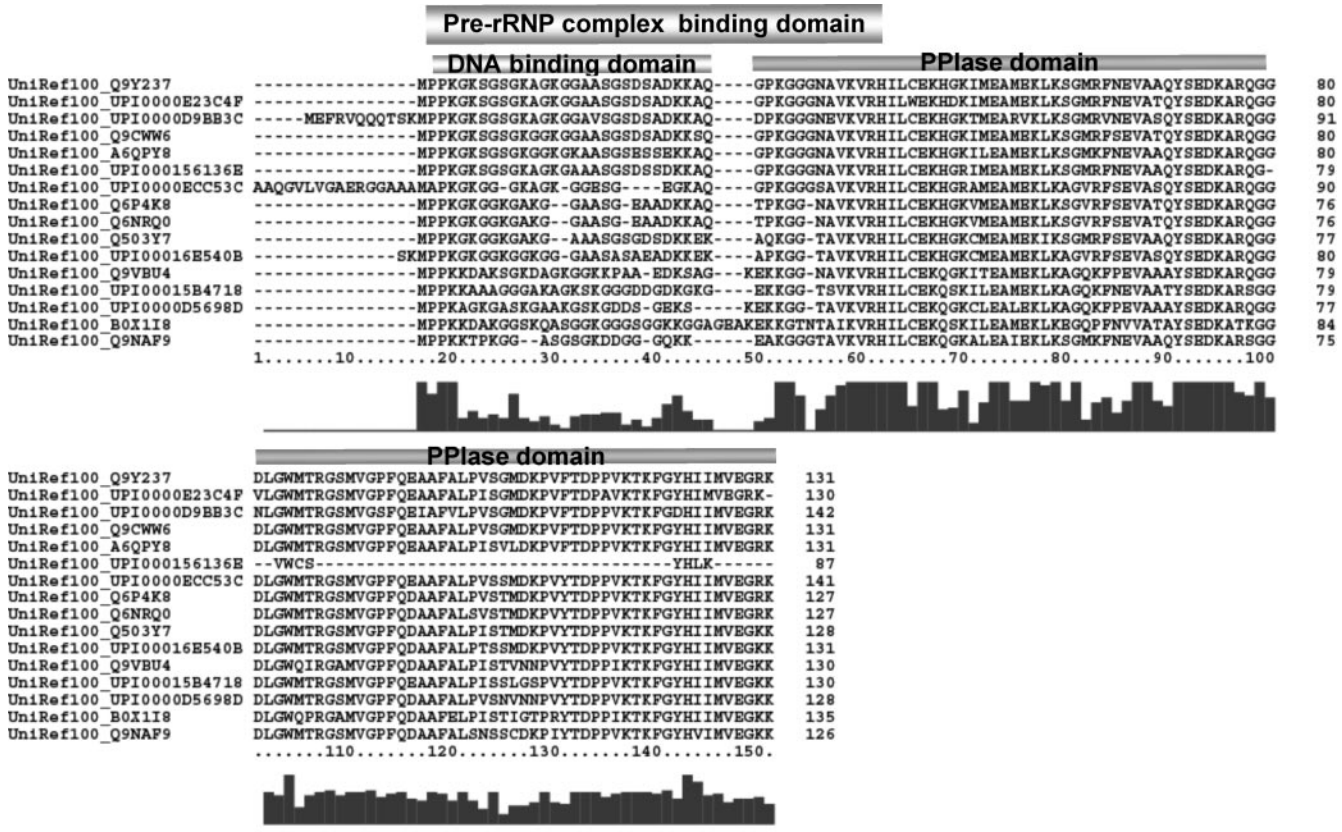

Taxonomy	UniRef Accession No.	Rep ID	identities (%)	similarities (%)	gaps (%)	match
Homo sapiens	UniRef100_Q9Y237	PIN4_HUMAN	100	100	-	6/6
Pan troglodytes	UniRef100_UPI0000E23C4F	UPI0000E23C4F	94	94	0	6/6
Macaca mulatta	UniRef100_UPI0000D9BB3C	UPI0000D9BB3C	90	91	-	5/6
Mus musculus	UniRef100_Q9CWW6	PIN4_MOUSE	96	97	-	6/6
Bos taurus	UniRef100_A6QPY8	A6QPY8_BOVIN	92	97	-	6/6
Equus caballus	UniRef100_UPI000156136E	UPI000156136E	96	98	-	6/6
Gallus gallus	UniRef100_UPI0000ECC53C	UPI0000ECC53C	83	89	4	5/6
Xenopus tropicalis	UniRef100_Q6P4K8	Q6P4K8_XENTR	87	92	3	6/6
Xenopus laevis	UniRef100_Q6NRQ0	Q6NRQ0_XENLA	86	91	3	6/6
Danio rerio	UniRef100_Q503Y7	Q503Y7_DANRE	82	88	2	5/6
Takifugu rubripes	UniRef100_UPI00016E540B	UPI00016E540B	82	88	1	5/6
Drosophila melanogaster	UniRef100_Q9VBU4	Q9VBU4_DROME	71	80	2	6/6
Nasonia vitripennis	UniRef100_UPI00015B4718	UPI00015B4718	71	79	0	4/6
Tribolium castaneum	UniRef100_UPI0000D5698D	UPI0000D5698D	70	79	2	5/6
Culex quinquefasciatus	UniRef100_B0X1I8	B0X1I8_CULQU	62	72	2	4/6
Caenorhabditis elegans	UniRef100_Q9NAF9	Q9NAF9_CAEEL	72	80	5	5/6

FIG. 6. **Alignment of the amino acid sequences of Par14 homologs in *H. sapiens*, *Pan troglodyte*, *Macaca mulatta*, *Mus musculus*, *Bos taurus*, *Equus caballus*, *Gallus gallus*, *Xenopus tropicalis*, *Xenopus laevis*, *Danio rerio*, *Takifugu rubripes*, *D. melanogaster*, *Nasonia vitripennis*, *Tribolium castaneum*, *Culex quinquefasciatus*, and *C. elegans*.** Gaps in alignment are represented by *dashes*. The pre-rRNP complex-binding domain, the DNA-binding domain, and the PPIase domain are indicated *above* the alignment. The accession number of each amino acid sequence is the NCBI GI number. The *numbers* indicated *below* the sequence alignment are those of the amino acid residues of the *Gallus gallus* sequence, and the *bar graph below* them represents the fractional identities of the aligned positions.

NNP18/NOPP34/hNIFK; Gene ID 67949 in Table I) is involved in cytokinesis as well as pre-rRNA processing (23) supports this proposal. It is known that nucleolar components involved in pre-rRNA processing, including incompletely processed pre-rRNA forms, are transferred from parental to daughter cell nucleoli by means of transient structures, such as the perichromosomal sheath and prenucleolar bodies; moreover a subset of these complexes does not disaggregate during cell division but rather remains intact and becomes incorporated into new nucleoli (19–22). Following mitosis, ribosome biogenesis can resume not only at the transcriptional level but also at intermediate levels of pre-rRNA processing. Par14 may be involved in these processes. Interestingly it has been suggested that phosphorylation of Par14 at Ser-19 is cata-

lyzed by casein kinase II, which is a regulator of mitosis (10). The fact that only the dephosphorylated form of Par14, Par14-b, binds to DNA in the nucleus and associates with pre-40 S and pre-60 S ribosomes suggests that phosphorylation/dephosphorylation at Ser-19 regulates its binding to not only DNA but also to the pre-rRNP complexes. Furthermore these data imply that Par14 binding to the pre-rRNP complexes may be regulated by casein kinase II and/or by its binding to DNA. Thus, our present results provide a molecular explanation to the report that phosphorylation of the amino-terminal domain regulates the subcellular localization and DNA binding properties of Par14 (10). Our data also support the idea that Par14 is involved in the coordinated redistribution of the pre-rRNP complexes and chromosomes during mitosis. That Par14 has apparently evolved in the metazoan lineage is consistent with the evolution of cell cytokinesis; namely animal species that have Par14 homologs including *Homo sapiens*, *Drosophila melanogaster*, and *Caenorhabditis elegans* require the central spindle to efficiently undergo cytokinesis (25, 26). It is very intriguing to speculate that the role of Par14 in ribosome biogenesis has evolved in conjunction with the cytokinesis-requiring central spindle.

The present study is in apparent disagreement with a previous report on the subcellular localization of Par14: Par14 was reported to be excluded from the nucleolus (10) based on experiments using Par14 tagged with either green fluorescent protein or histidine in contradiction to our current results. We also note that Par14 tagged with FLAG at either the amino or carboxyl terminus tended to be excluded from the nucleolus and became dispersed throughout the nucleoplasm, whereas endogenous Par14 was clearly concentrated in the nucleolus (Fig. 1*A*). In addition, when we attempted to pull down Par14-associated proteins using FLAG-tagged Par14 expressed in cells, FLAG-Par14 did not specifically associate with other proteins (supplemental Fig. 5A) or with preribosomal fractions of nuclear extract (supplemental Fig. 5B). We consider it likely that these results reflect an altered specificity of FLAG-Par14 compared with that using other tags: the FLAG tag (DYKDDDDK) has a net negative charge that may affect the binding of Par14 to the pre-rRNP complexes. Nonetheless exogenously expressed Par14 differs from the endogenous protein in terms of cellular localization and preferential binding partners in the cell. It is not impossible that exogenous expression of tagged Par14 induces some form of cellular stress, thereby causing qualitative changes in the pre-rRNP complexes and/or nucleolar structure. However, the most probable explanation is that our results reflect the behavior of endogenous Par14 in the cell; the successful isolation of the pre-rRNP complexes in our study is attributable to the use of affinity-purified recombinant Par14 as the affinity bait because affinity-purified GST-Par14 has not undergone any primary post-translational modifications. Thus, the biochemical nature of Par14 implicates its unique biological roles in ribosome biogenesis as well as in connecting the pre-rRNP complexes with DNA during ribosome biogenesis and/or events related thereto.

Acknowledgment—We thank Dr. D. Stavreva (NCI, National Institutes of Health) for valuable discussions and suggestions.

* This work was supported in part by the Japan Health Science Foundation (H18-Soyaku-Ippan-001) (to N. T.), by research fellowships of the Japan Society for the Promotion of Science (to S. F.-N.), and by the Targeted Proteins Research Program from the Ministry of Education, Culture, Sports, Science and Technology (MEXT), Japan (to K. H.).

S The on-line version of this article (available at http://www.mcponline.org) contains supplemental material.

[b] Both authors contributed equally to this work.

[c] Present address: Inst. of Molecular and Cellular Biosciences, The University of Tokyo, 1-1-1 Yayoi, Bunkyo-ku, Tokyo 113-0032.

[f] Present address: Dept. of Bioscience and Bioinformatics, College of Information Science and Engineering, Ritsumeikan University, 1-1-1 Nojihigashi, Kusatsu 525-8577, Japan.

[j] To whom correspondence should be addressed: Applied Biological Science, Tokyo University of Agriculture and Technology, 3-5-8 Saiwai-cho, Fuchu, Tokyo 183-8509, Japan. Fax: 81-042-367-5709; E-mail: ntakahas@cc.tuat.ac.jp.

REFERENCES

1. Fischer, G., Tradler, T., and Zarnt, T. (1998) The mode of action of peptidyl prolyl cis/trans isomerase in vivo: binding vs. catalysis. *FEBS Lett.* **426,** 17–20
2. Takahashi, N. (2002) Mode of action of FK506 and rapamycin, in *Macrolide Antibiotics II: Chemistry, Biology and Practice* (Omura, S., ed.) pp. 577–621, Academic Press, New York
3. Shieh, B. H., Stamnes, M. A., Seavello, S., Harris, G. L., and Zuker, C. S. (1989) The *ninaA* gene required for visual transduction in Drosophila encodes a homologue of cyclosporin A-binding protein. *Nature* **338,** 67–70
4. Pennisi, E. (1996) Expanding the eukaryote's cast of chaperones. *Science* **274,** 1613–1614
5. Takahashi, N., Hayano, T., and Suzuki, M. (1989) Peptidyl-prolyl cis-trans isomerase is the cyclosporin A-binding protein cyclophilin. *Nature* **337,** 473–475
6. Siekierka, J. J., Hung, S. H., Poe, M., Lin, C. S., and Sigal, N. H. (1989) A cytosolic binding protein for the immunosuppressant FK506 has peptidyl-prolyl isomerase activity but is distinct from cyclophilin. *Nature* **341,** 755–757
7. Maki, N., Sekiguchi, F., Nishimaki, J., Miwa, K., Hayano, T., Takahashi, N., and Suzuki, M. (1990) Complementary DNA encoding the human T-cell FK506-binding protein, a peptidyl prolyl cis-trans isomerase distinct from cyclophilin. *Proc. Natl. Acad. Sci. U.S.A.* **87,** 5440–5443
8. Rulten, S., Thorpe, J., and Kay, J. (1999) Identification of eukaryotic parvulin homologues: a new subfamily of peptidylprolyl cis-trans isomerases. *Biochem. Biophys. Res. Commun.* **259,** 557–562
9. Uchida, T., Fujimori, F., Tradler, T., Fischer, G., and Rahfeld, J. U. (1999) Identification and characterization of a 14 kDa human protein as a novel parvulin-like peptidyl prolyl cis/trans isomerase. *FEBS Lett.* **446,** 278–282
10. Reimer, T., Weiwad, M., Schierhorn, A., Ruecknagel, P. K., Rahfeld, J. U., Bayer, P., and Fischer, G. (2003) Phosphorylation of the N-terminal domain regulates subcellular localization and DNA binding properties of the peptidyl-prolyl cis/trans isomerase hPar14. *J. Mol. Biol.* **330,** 955–966
11. Sekerina, E., Rahfeld, J. U., Müller, J., Fanghänel, J., Rascher, C., Fischer, G., and Bayer, P. (2000) NMR solution structure of hPar14 reveals similarity to the peptidyl prolyl cis/trans isomerase domain of the mitotic regulator hPin1 but indicates a different functionality of the protein. *J. Mol. Biol.* **301,** 1003–1017
12. Fujiyama, S., Yanagida, M., Hayano, T., Miura, Y., Isobe, T., Fujimori, F., Uchida, T., and Takahashi, N. (2002) Isolation and proteomic characterization of human parvulin associating preribosomal ribonucleoprotein complexes. *J. Biol. Chem.* **277,** 23773–23780

13. Takahashi, N., Yanagida, M., Fujiyama, S., Hayano, T., and Isobe, T. (2003) Proteomic snapshot analysis of preribosomal ribonucleoprotein complexes formed at various stages of ribosome biogenesis in yeast and mammalian cells. *Mass Spectrom. Rev.* **22,** 287–317
14. Natsume, T., Yamauchi, Y., Nakayama, H., Shinkawa, T., Yanagida, M., Takahashi, N., and Isobe, T. (2002) A direct nanoflow liquid chromatography-tandem mass spectrometry system for interaction proteomics. *Anal. Chem.* **74,** 4725–4733
15. Hayano, T., Yanagida, M., Yamauchi, Y., Shinkawa, T., Isobe, T., and Takahashi, N. (2003) Proteomic analysis of human Nop56p-associated pre-ribosomal ribonucleoprotein complexes: possible link between Nop56p and the nucleolar protein treacle responsible for Treacher Collins syndrome. *J. Biol. Chem.* **278,** 34309–34319
16. Yanagida, M., Hayano, T., Yamauchi, Y., Shinkawa, T., Natsume, T., Isobe, T., and Takahashi, N. (2004) Human fibrillarin forms a sub-complex with splicing factor 2-associated p32, protein arginine methyltransferases, and tubulins alpha 3 and beta 1 that is independent of its association with preribosomal ribonucleoprotein complexes. *J. Biol. Chem.* **279,** 1607–1614
17. Shinkawa, T., Taoka, M., Yamauchi, Y., Ichimura, T., Kaji, H., Takahashi, N., and Isobe, T. (2005) STEM: a software tool for large-scale proteomic data analyses. *J. Proteome Res.* **4,** 1826–1831
18. Nunomura, K., Nagano, K., Itagaki, C., Taoka, M., Okamura, N., Yamauchi, Y., Sugano, S., Takahashi, N., Izumi, T., and Isobe, T. (2005) Cell surface labeling and mass spectrometry reveals diversity of cell-surface markers and signaling molecules expressed in undifferentiated mouse embryonic stem cells. *Mol. Cell. Proteomics* **4,** 1968–1976
19. Medina, F. J., Cerdido, A., and Fernández-Gómez, M. E. (1995) Components of the nucleolar processing complex (pre-rRNA, fibrillarin, and nucleolin) colocalize during mitosis and are incorporated to daughter cell nucleoli. *Exp. Cell Res.* **221,** 111–125
20. Gautier, T., Fomproix, N., Masson, C., Azum-Gélade, M. C., Gas, N., and Hernandez-Verdun, D. (1994) Fate of specific nucleolar perichromosomal proteins during mitosis: cellular distribution and association with U3 snoRNA. *Biol. Cell* **82,** 81–93
21. Lerch-Gaggl, A., Haque, J., Li, J., Ning, G., Traktman, P., and Duncan, S. A. (2002) Pescadillo is essential for nucleolar assembly, ribosome biogenesis, and mammalian cell proliferation. *J. Biol. Chem.* **277,** 45347–45355
22. Olson, M. O., and Dundr, M. (2005) The moving parts of the nucleolus. *Histochem. Cell Biol.* **123,** 203–216
23. Oeffinger, M., and Tollervey, D. (2003) Yeast Nop15p is an RNA-binding protein required for pre-rRNA processing and cytokinesis. *EMBO J.* **22,** 6573–6583
24. Young, D. W., Hassan, M. Q., Pratap, J., Galindo, M., Zaidi, S. K., Lee, S. H., Yang, X., Xie, R., Javed, A., Underwood, J. M., Furcinitti, P., Imbalzano, A. N., Penman, S., Nickerson, J. A., Montecino, M. A., Lian, J. B., Stein, J. L., van Wijnen, A. J., and Stein, G. S. (2007) Mitotic occupancy and lineage-specific transcriptional control of rRNA genes by Runx2. *Nature* **445,** 442–446
25. McCollum, D. (2004) Cytokinesis: the central spindle takes center stages. *Curr. Biol.* **14,** R953–955
26. D'Avino, P. P., Savoian, M. S., and Glover, D. M. (2005) Cleavage furrow formation and ingression during animal cytokinesis: a microtubule legacy. *J. Cell Sci.* **118,** 1549–1558
27. Fatica, A., and Tollervey, D. (2002) Making ribosomes. *Curr. Opin. Cell Biol.* **14,** 313–318